Int. J. Multiphase Flow Vol. 17, No. 6, pp. 783–803, 1991
Printed in Great Britain.

0301-9322/91 $3.00 + 0.00

THE DRAINAGE AND RUPTURE OF A NON-FOAMING LIQUID FILM FORMED UPON BUBBLE IMPACT WITH A FREE SURFACE

L. DOUBLIEZ
Ecole Nationale Supérieure de Mécanique, 1 rue de la Noë, 44072 Nantes Cedex, France

(Received 15 July 1990; in revised form 5 June 1991)

Abstract—Experiments are performed to measure the thickness of a thin liquid film formed between a free surface and the apex of a bubble which is approaching at its terminal velocity. Measurements are made using bubbles of < 1 mm dia both in distilled water and alcoholic solutions (methanol, ethanol). The results of the experiments show that the models based on the lubrication approximation fail to predict the initial stage of drainage. A better agreement is obtained by modifying the model proposed by Chesters.

Key Words: bubble, coalescence, thin liquid film, drainage, rupture thickness

1. INTRODUCTION

The coalescence of bubbles plays an important part in many areas of interest to industry. It leads to a decrease in interfacial area in mass transfer equipment (e.g. bubble columns and air-lift reactors). In two-phase flow in pipes, the transition between bubble and slug flows depends on coalescence. A basic idea often used to model the coalescence process is to compare the time it takes to thin the intervening film between two bubbles (or two drops) to the rupture thickness with the contact time between these two bubbles (or two drops); see, for example: Thomas (1981) for bubbles; and Coualaloglou & Tavlarides (1977) and Das *et al.* (1987) for drops.

There exist numerous theoretical and experimental investigations appertaining to the film drainage, particularly for foam films. For a recent review see, for example, Ivanov & Dimitrov (1988); and for more recent works: Hahn *et al.* (1985), Oolman & Blanch (1986), Chen & Slattery (1988), Davis *et al.* (1989), Yiantsios & Davis (1990) and Prince & Blanch (1990a). Most of the models of the aforementioned studies are based on the lubrication approximation theory, namely the quasi-static assumption which neglects the inertia terms in the equations of motion. But for other authors, the viscosity is not the main factor and can even be neglected. Here drainage times are predicted to be several orders of magnitude shorter. In fact, the choice of the leading terms in the governing equations is connected with the boundary conditions at the film surfaces which can be tangentially mobile or immobile in the presence of surfactant.

For non-foaming liquids, not many experimental data are available. Most experimental studies involve the observation of a large population of bubbles and knowledge of the coalescence process is only indirect via interfacial area or hold-up. For solutes like electrolytes or organic compounds like alcohols, the main feature is that there is a sharp transition between the quick coalescence which occurs in pure water and a coalescence inhibition which takes place in a narrow concentration range (Zieminski & Whittemore 1971; Keitel & Onken 1982; Prince & Blanch 1990b). Direct study of coalescence is easier with measurement on an isolated bubble pair, or with a bubble approaching a free surface. With two bubbles growing side by side at the tip of two capillary tubes, it is possible to obtain a coalescence probability from the percentage of pairs of bubbles which coalesce before their detachment from the tubes (Lessard & Zieminski 1971; Kim & Lee 1988). The coalescence time is then defined as the lifetime of the lamella created between the two bubbles (Nicodemo *et al.* 1972; Sagert *et al.* 1976; Drogaris & Weiland 1983; Yang & Maa 1984). The film thicknesses can also be measured by the technique described herein (Allan *et al.* 1961; Cain & Lee 1985).

Various theories have been proposed to explain the effect of solutes: a gradient of surface tension which imparts a partial immobility to the interface (Lee & Hodgson 1968); an increase in surface tension due to stretching (Andrew 1960) which can be relaxed by a diffusion process at the film border (Marrucci 1969); and structural changes in the solvent water caused by dissolved electrolytes (Zieminski & Whittemore 1971). The variation of the critical thickness at which the film breaks may be also invoked (Ruckenstein & Sharma 1987; Sharma & Ruckenstein 1987).

Owing to the diversity of theoretical assumptions, it is necessary to obtain a more complete data set on the drainage process, such as rate of thinning and rupture thickness, and to compare these with the values predicted by the models. For non-foaming liquids (i.e. when there are no double-layer repulsion or steric effects to stabilize the film), the lifetimes of the lamellae are short (<1 s); in such cases there is a lack of experimental data. Only Cain & Lee (1985), to our knowledge, have reported thickness measures on fast drainage of a film between two captive bubbles in KCl solutions. In addition, the experiments of Kirkpatrick & Lockett (1974) have demonstrated that the approach velocity is an important factor in limiting bubble coalescence.

In order to investigate the applicability of the models in the literature for non-foaming liquids and for bubbles having a definite approach velocity, we describe an apparatus to measure the thickness of the film between a free surface and the apex of a bubble approaching at its terminal velocity. Measurements are then made using distilled water and alcoholic solutions (methanol, ethanol). The inhibition of coalescence by these alcohols has already been studied in bubble columns (Keitel & Onken 1982) or with contacted pairs of bubbles (Sagert *et al.* 1976; Drogaris & Weiland 1983). The aim of the present work is to determine whether the inhibition is due to slower rate of drainage, smaller thickness of rupture or greater stability of the surfaces of the intervening film with addition of alcohol. The results show that both the drainage and rupture are more complex that one would expect.

2. EXPERIMENT

The thickness measurement is based on the examination of interference fringes shifts. The technique is similar to that used by Allan *et al.* (1961).

A bubble is formed in a beaker at the tip of a capillary tube by blowing nitrogen from a gas bottle at a rate of <1 bubble/s (figure 1). The tip is approx. 5 cm below the surface. The tube is fixed onto an arm which can be accurately positioned on the optic axis of a metallurgical microscope by means of micrometer screws. The volume of the bubbles can be well-reproduced and is determined by collecting a fixed number of bubbles with a calibrated pipette. Different bubble volumes are obtained by changing the capillary.

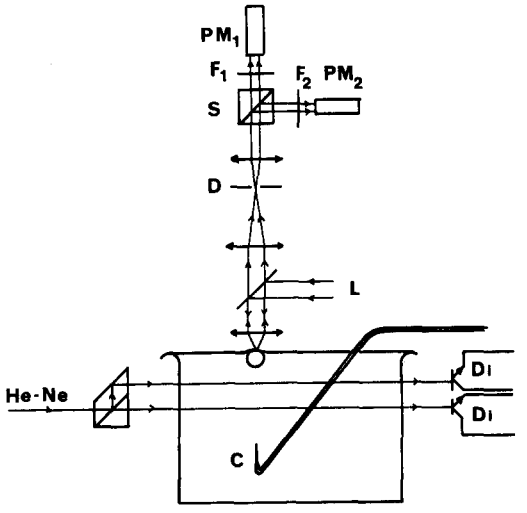

Figure 1. Experimental apparatus: C, capillary tube; D, diaphragm; Di, photodiode; F_1, F_2, interference filters; PM_1, PM_2, photomultiplier tubes; S, beam splitter; L, mercury vapour lamp; He–Ne, laser beam.

Table 1. Values of the reflection coefficient R corresponding to coincidences of maximum or minimum of light intensity

$\lambda = 436$ nm		$\lambda = 546$ nm		$\lambda = 578$ nm	
hn(nm)	R	hn(nm)	R	hn(nm)	R
0	0	0	0	0	0
436	0			433	1
545	1	546	1		
872	0			866	0
1090	0	1092	0		

h = Film thickness; n = refractive index of the liquid.

Before reaching the surface, a bubble crosses two horizontal parallel beams 2 cm apart. The passage through the beams is detected by two photodiodes. The rise velocity is deduced from the transit time and thus the value of the bubble volume may be checked since the two are correlated.

The beaker stays on a platform which is mounted onto a vibration-insulated granite table and which can be moved vertically. The free surface lies in the focal plane of the objective lens of the microscope. The surface immobility before the impact of a bubble was controlled by examination of a laser beam reflected onto it.

The source of illumination is a high intensity mercury vapour lamp (200 W). The film thickness is deduced from the intensity of the reflected light using the classical formula (Scheludko 1967):

$$R = \frac{I}{I_{max}} = \frac{(1+r^2)^2 \sin^2\left(\frac{2\pi hn}{\lambda}\right)}{1 - 2r^2 \cos\left(\frac{4\pi hn}{\lambda}\right) + r^4}, \quad [1]$$

where

I = reflected intensity,

I_{max} = maximum reflected intensity,

r = reflection coefficient of the liquid,

n = refractive index of the liquid,

h = film thickness

and

λ = wavelength of incident light.

With a monochromatic light, the intensity I is a periodic function of period $\lambda/2n$, and the interference order is unknown unless a reference thickness is available. With white light, the interference pattern is coloured, and the order may be estimated from standard tables of colours. In our experiments, the drainage time is <5 ms and classic video or cine-cameras cannot be used to record the pattern. Also, we choose to analyse the reflected light at two wavelengths λ and λ' with two photomultiplier tubes (PM_1, PM_2). These wavelengths are selected by two interference filters (F_1, F_2) placed in front of the photomultiplier tubes. For λ, we took the mercury line 436 nm, and for λ' we used either 546 nm (λ'_1) or 578 nm (λ'_2). For some thicknesses, the I_λ and $I_{\lambda'}$ curves go simultaneously through an extremum. The thicknesses corresponding to these coincidences are given in table 1 and are used as reference thicknesses. We have observed that the film thickness h does not decrease during all of the residence time of the bubble at the free surface, but that the bubble has a vertical movement of oscillation after impact at the free surface. Also thinning and thickening of the intervening film can alternate. The reversal of the thinning rate appears on the intensity curves as an extremum which generally is neither a minimum nor a maximum. For example, figure 2 shows the intensities I_λ, $I_{\lambda'_1}$ and $I_{\lambda'_2}$ corresponding to a typical draining curve $h(t)$. The reversal at $t = t_r$ for $hn = 545$ nm is obvious for $I_{\lambda'_2}$, but if one examines only I_λ or $I_{\lambda'_1}$, there is a certain ambiguity since this thickness gives a maximum or a minimum for the reflected intensities. This is the reason why we simultaneously used two wavelengths with the ability to change the interference filters. The currents provided by photomultipliers are converted by an operational amplifier to a voltage which is recorded by a digital oscilloscope at a sampling rate up to 1 MHz. A circular aperature is placed into the image plane so that the photomultipliers receive light from a film area of 10 μm dia.

Before each experiment, the beaker was soaked in a hot nitric and sulphuric acid mixture. It was rinsed several times in tap water and then in distilled water. The free surface was renewed by overflowing just before each measurement in order to minimize surface contamination. The solutions used were prepared with de-ionized and distilled water and with analytical grade reagents.

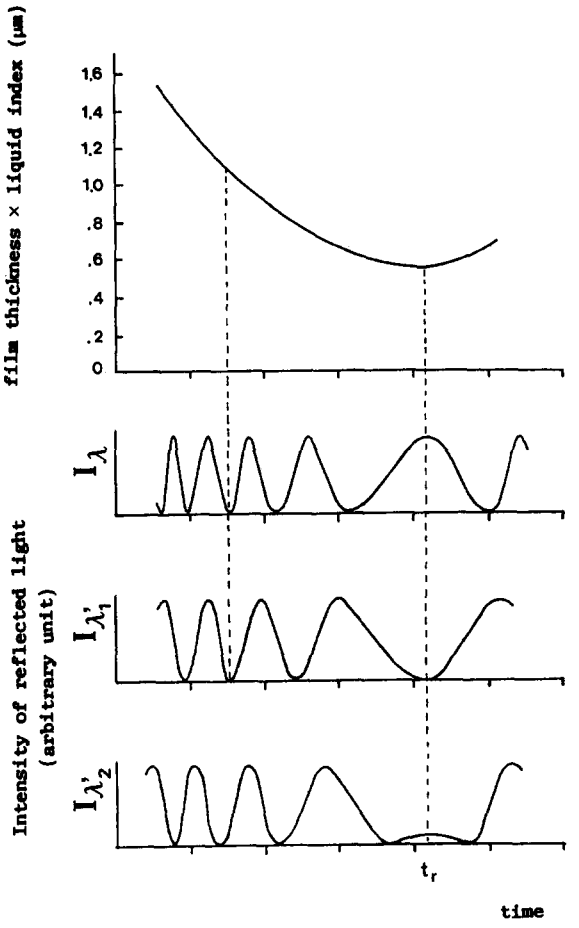

Figure 2. Schematic representation of light intensity curves $I_\lambda(t)$, $I_{\lambda'_1}(t)$ and $I_{\lambda'_2}(t)$ corresponding to a typical drainage curve $h(t)$ (multiplied by the liquid index n); $\lambda = 436$ nm, $\lambda'_1 = 546$ nm, $\lambda'_2 = 578$ nm.

3. RESULTS

Thickness measurements were made with bubble radii ranging from 0.27 to 0.43 mm, so that the rising motion is rectilinear and the impact point at the free surface does not randomly change too much in the focal plane of the microscope.

Bouncing

Typical intensity curves $I_\lambda(t)$ and $I_{\lambda'}(t)$ and the deduced thickness vs time curve $h(t)$ are shown in figure 3. One can see that the bubble rebounds twice before bursting. The three interference fringes sets are given by the three approaches. The last one results in the film rupture. If the residence time is the interval of time between the first arrival of a bubble at a free surface and its bursting, and if the drainage time is the interval of time to thin the film from an initial definite thickness to the rupture thickness, we see that residence time and drainage time are well-distinguished.

The number of bounces depends on the bubble volume and on the alcohol concentration. With distilled water, the bubbles burst at the first contact with the free surface if their diameter is $\lesssim 0.65$ mm. Between 0.65 and 1 mm, the bubbles bounce one time and burst at the next approach. For a diameter a little greater than 1 mm, the bubbles burst at the third approach. This has been already observed by Farooq (1972). Kirkpatrick & Lockett (1974) also noticed that bubbles (equivalent dia = 5 mm) sink into the interface without coalescence and then oscillate at the surface before finally coalescing. Transitions between bursting and bouncing are not sharp. For a series of bubbles corresponding to a limit of these ranges, we observe that a fraction burst and the remainder bounce. The ratio value is very sensitive to the surface contamination. The probability

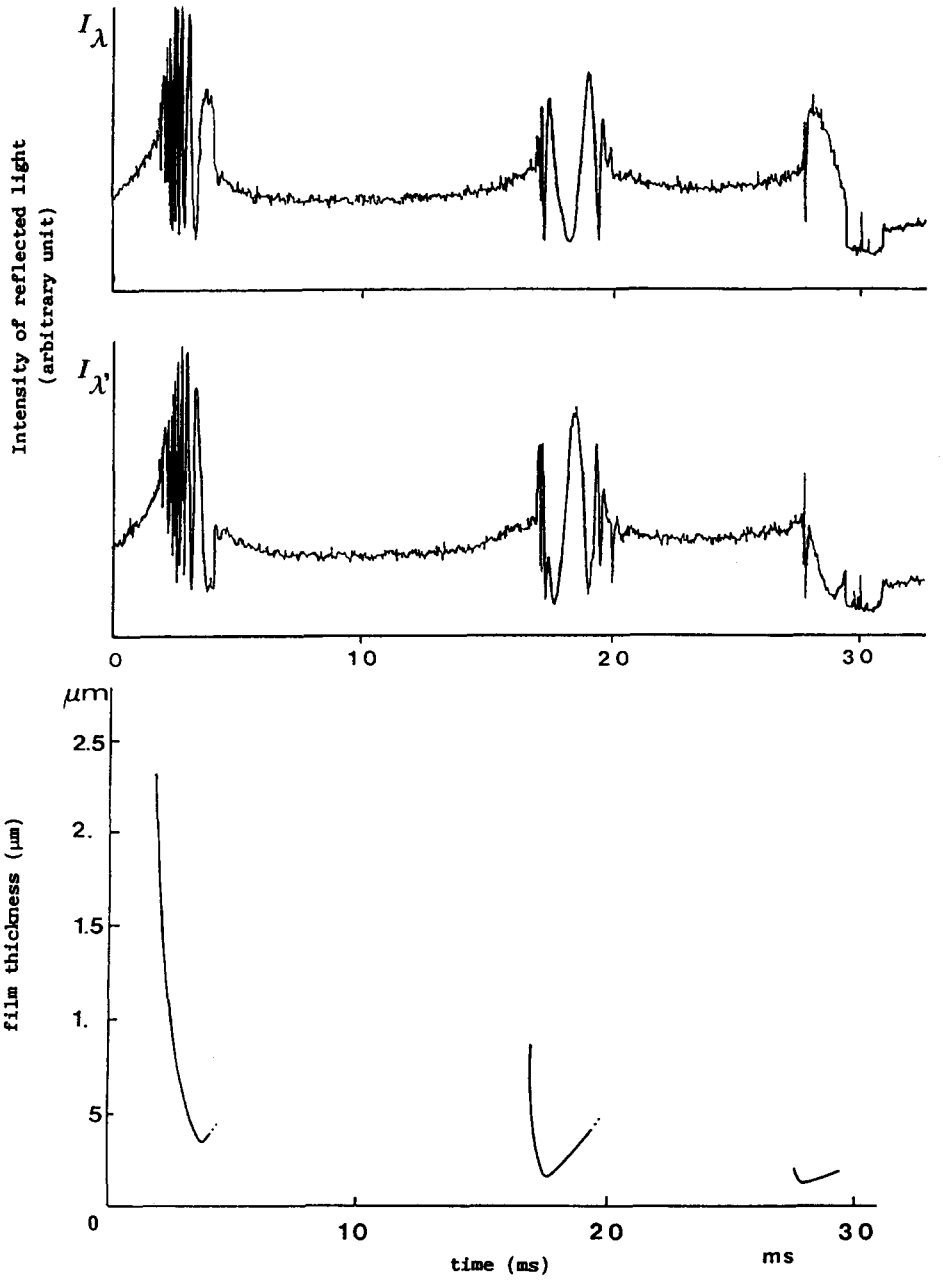

Figure 3. Experimental light intensity curves I_λ and $I_{\lambda'}$ with the deduced thickness; ethanol concentration = 0.2 mol/l, bubble dia = 0.85 mm, terminal velocity = 0.22 m/s.

of a rebound increases with the surface ageing. With the addition of alcohol (methanol, ethanol) we also observe an increase in the number of bounces and accordingly the residence time is longer, as may be seen in figure 4.

Thickness

The thickness measurements are very reproducible when the cleaning procedure is repeated before each experiment. The results in figure 5 are taken from six runs with distilled water and correspond to the first approach. Two bubbles burst during this approach; the other four bounce and burst at the next approach. As may be seen, the shape of the drainage curves remains the same whether the film breaks or not. The thickness vs time curves exhibit three stages: a fast drainage; a reduced rate and an arrest of the thinning; and finally, a thickening of film. The most striking observation is that if bursting occurs, the film rupture more often takes place during the last stage

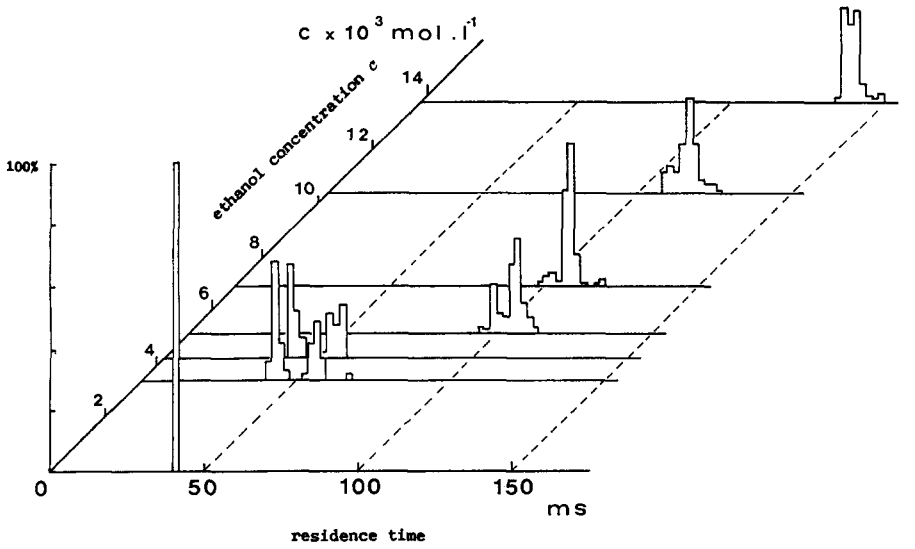

Figure 4. Histogram of residence times for aqueous solutions of ethanol; bubble volume = 0.6 mm³.

when the thickness is increasing. The thicknesses at the rupture point are large in comparison with those observed with foaming liquids. For the six runs in figure 5, the values are 340 and 435 nm for the two bubbles bursting at the first impact and range from 110 to 150 nm for the others. We have never observed rupture thickness of <80 nm for our experiments with distilled water and alcoholic solutions. If the microscope axis is moved off the centre of the film, the draining curves

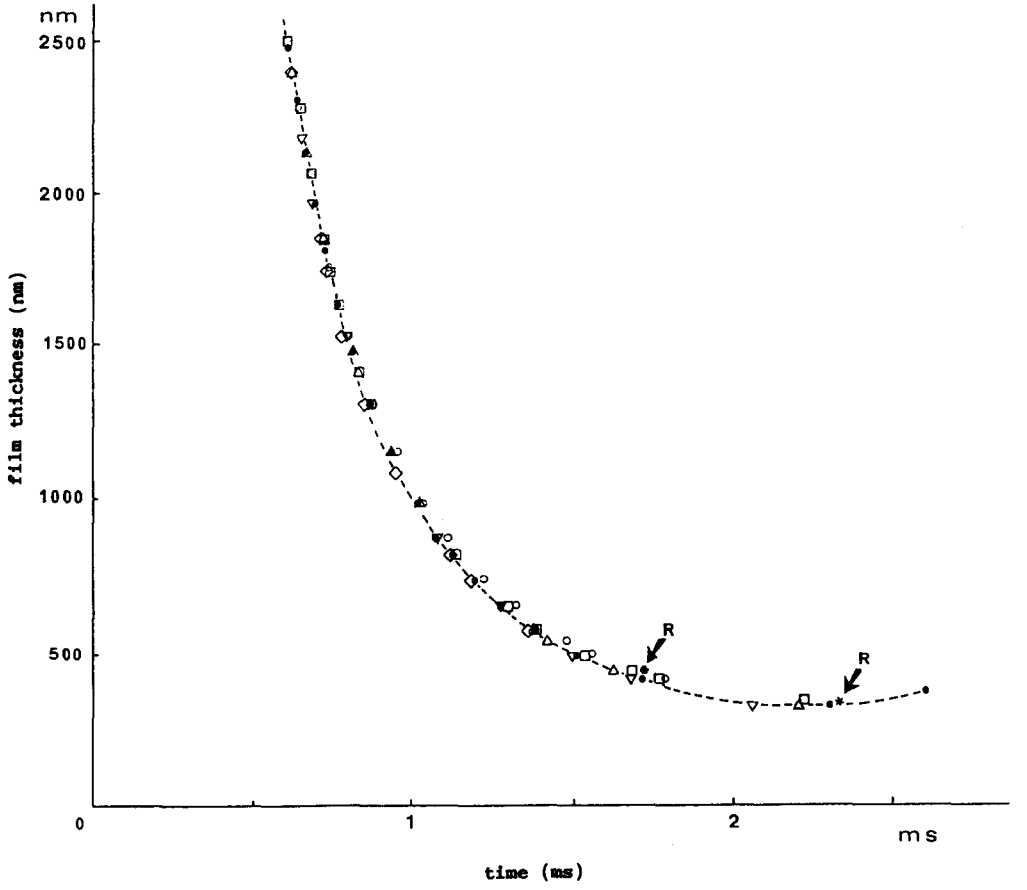

Figure 5. Film thickness vs time for six runs with distilled water: two bubbles burst (R), the other four bounce and burst at the next oscillation; bubble volume = 0.25 mm³, terminal velocity = 0.19 m/s.

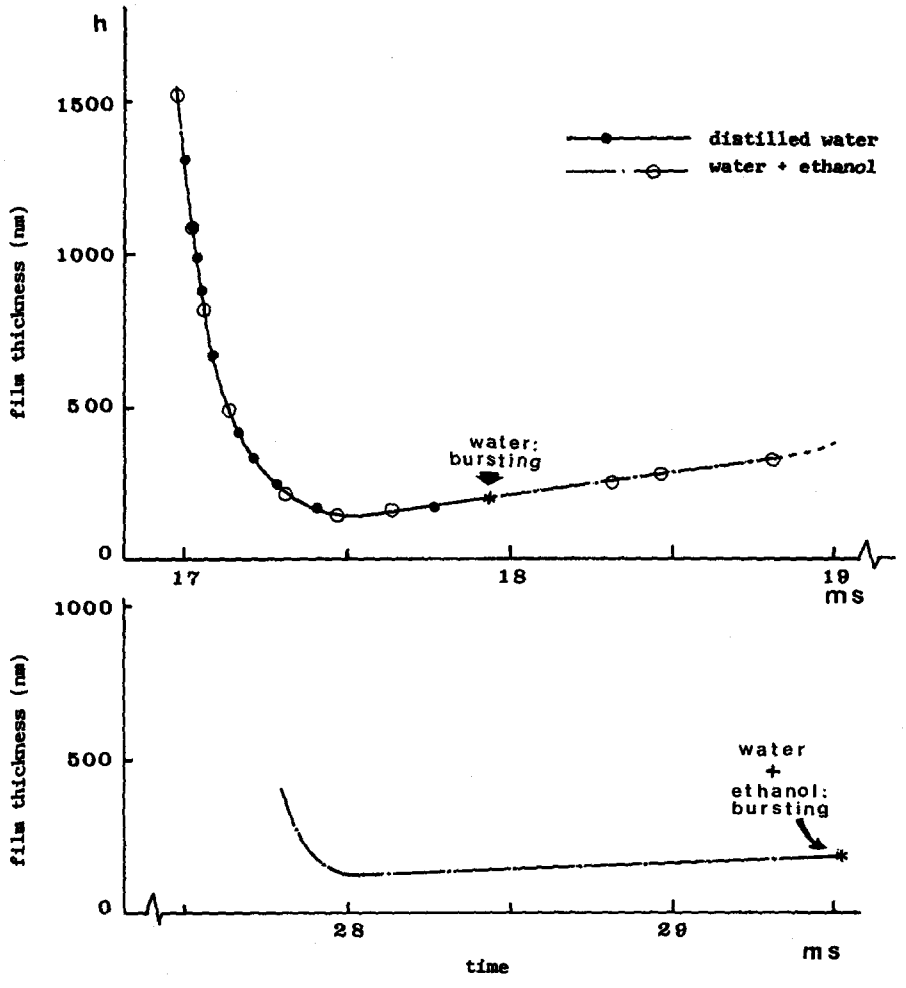

Figure 6. Comparison of drainage curves in distilled water and in an aqueous solution of ethanol ($3.4 \cdot 10^{-3}$ mol/l). In water, the film breaks at $t = 18$ ms (upper curve); in the alcoholic solution, the bubble bursts at the next oscillation, $t = 29.5$ ms (lower curve). It is the same run as in figure 3.

remain similar. The contrast is conserved when the diameter of the examined area is multiplied by four by changing the microscope magnification. Thus, we believe that the thickness is uniform in the main part of the film and that perhaps it is thinner at the rim, but it is difficult to obtain measurements there on account of the rapid variation of the curvature. It is likely that the thickness at the moment of rupture is not the rupture thickness, if the latter means the thickness at the point where the film breaks. For foams, during film formation, a stage is often observed where the surface acquires a bell-shape form called a dimple. The radial flow in the film then is inverted and the thickness increases at the centre while the film thins at the border.

It must be pointed out that for clean surfaces we do not observe a growth of instabilities with measurements performed on an area of 10 μm dia and at a sampling rate of 1 MHz. These instabilities are often postulated to explain the rupture.

When either methanol or ethanol are added in low concentration ($3.4 \cdot 10^{-3}$ mol/l), such that the physical properties like density, viscosity, surface tension are little affected, the film behaves in the same way as for contaminated water: the drainage curves are the same as for distilled water but instead of observing the film rupture one can see, in figure 6, that the film continues to thicken; the bubble bounces and the rupture occurs at the next approach. Thus, the coalescence inhibition by alcohol is not associated with a modification of the central film drainage rate.

Thinning rate

When the drainage curves are compared for the successive approaches of a bubble, it may be seen for a given thickness during the first stage of drainage that the thinning rate is higher for the

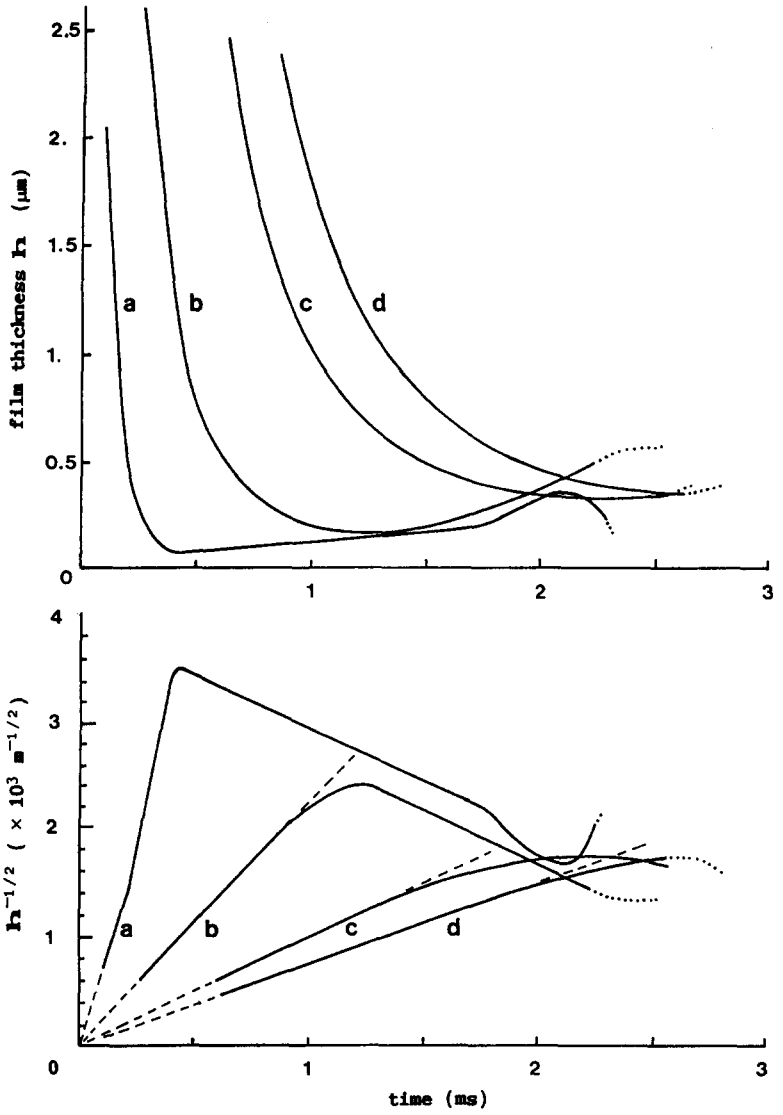

Figure 7. Film thickness h and corresponding $h^{-1/2}$ values vs t for the first approach of bubbles of various diameter:

Bubble	Dia (mm)	Terminal velocity (m/s)
a	0.54	0.11
b	0.70	0.17
c	0.78	0.19
d	0.85	0.22

second bounce than for the first, and higher for the third than for the second. In comparing the first approaches of bubbles of various volumes, it is seen that the thinning rate decreases with the rising velocity which increases with the volume. Also, it may be concluded that the higher the approach velocity is, the slower is the initial thinning rate.

In figure 7, values of $h^{-1/2}$ are plotted vs t and exhibit a linear relationship during the initial stage. This relationship is not consistent with the classical Reynolds model based on a plane film, together with the lubrication approximation. The Reynolds velocity is given by

$$V_{Re} = -\frac{dh}{dt} = \frac{2Fh^3}{3\pi\mu R_f^4}, \qquad [2]$$

where

F = total force acting on the film,

μ = dynamic viscosity

and

R_f = film radius.

If the experimental law

$$h^{-1/2} = \alpha t \qquad [3]$$

is assumed in [2], the film radius must vary with time as

$$R_f^4 = \frac{F}{3\pi\mu\alpha} h^{3/2}. \qquad [4]$$

Here $F = \pi R_f^2 \Delta P$, where ΔP is the capillary pressure, which for a bubble at a free surface (Lee & Hodgson 1968) is given by

$$\Delta P = \frac{\gamma}{R_b}, \qquad [5]$$

where γ is the interfacial tension. Substituting [5] in [4], the film radius may be expressed as

$$R_f^2 = \frac{\Delta P}{3\mu\alpha} h^{3/2}, \qquad [6]$$

implying that the film radius should decrease with the thickness during the approach.

In the Reynolds model, the surfaces are supposed to be tangentially immobile. The same dependence on the film radius is given by a similar analysis, where surface mobility is due to the effects of surface viscosity or of bulk and surface diffusion (Manev *et al.* 1984). In contrast to the lubrication hypothesis, Marrucci (1969) and Kirkpatrick & Lockett (1974) neglect viscosity effects and apply the Bernoulli equation between the centre of film and its rim. In the case of a bubble at a free surface, they obtain the following drainage equation for a plane-parallel film:

$$\frac{dh}{dt} = -\frac{2h}{R_f}\left(\frac{2\gamma}{\rho R_f}\right)^{1/2}. \qquad [7]$$

But use of the Bernoulli equation implies a steady flow and this assumption does not seem justified, as will be shown later.

Chesters (1975, 1978), assuming a plug flow in the plane film and taking account of the bubble velocity, gives the following expression for the thinning rate:

$$\frac{dh}{dt} = -\frac{8\gamma}{\rho V R_{eq}^2} h, \qquad [8]$$

where V is the approach velocity and for two bubbles of radii R_1 and R_2,

$$\frac{1}{R_{eq}} = \frac{1}{2}\left(\frac{1}{R_1} + \frac{1}{R_2}\right). \qquad [9]$$

Thus, for a bubble rising to a plane surface, assuming V constant and an initial thickness h_0 at $t = 0$:

$$t = \frac{\rho V R_{eq}^2}{8\gamma} \ln\left(\frac{h_0}{h}\right). \qquad [10]$$

This dependence is not what we observed during the first stage of drainage. We shall now show that [3] can be obtained by modifying the boundary conditions of Chester's (1975, 1978) model.

4. THINNING MODEL FOR THE FIRST STAGE OF DRAINAGE

We consider two bubbles of equal radii R moving towards one another along the line joining their centres with a relative velocity V_0. The hypotheses are:

(a) The intervening film is plane-parallel.
(b) Gravity effects can be neglected in the film flow.
(c) The flow is axisymmetric without an azimuthal component.
(d) The gas flow in the bubbles has no influence on the liquid flow.
(e) The radial velocity u is constant across the film: $(\partial u/\partial z = 0)$.

The last assumption will be discussed later. The continuity and Navier–Stokes equations are in cylindrical coordinates [with hypothesis (c)]:

$$\frac{1}{r}\frac{\partial(ur)}{\partial r} + \frac{\partial w}{\partial z} = 0, \qquad [11]$$

$$\frac{\partial u}{\partial t} + u\frac{\partial u}{\partial r} + w\frac{\partial u}{\partial z} = -\frac{1}{\rho}\frac{\partial p}{\partial r} + \frac{\mu}{\rho}\left[\frac{\partial}{\partial r}\left(\frac{1}{r}\frac{\partial(ru)}{\partial r}\right) + \frac{\partial^2 u}{\partial z^2}\right] \qquad [12]$$

and

$$\frac{\partial w}{\partial t} + u\frac{\partial w}{\partial r} + w\frac{\partial w}{\partial z} = -\frac{1}{\rho}\frac{\partial p}{\partial z} + \frac{\mu}{\rho}\left(\frac{\partial^2 w}{\partial r^2} + \frac{1}{r}\frac{\partial w}{\partial r} + \frac{\partial^2 w}{\partial z^2}\right), \qquad [13]$$

where u and w are the radial and axial velocities, respectively, p is the pressure, ρ is the liquid density and μ is the dynamic viscosity.

If L and H are characteristic lengths for the radial and axial directions, and U and W are the corresponding velocity scales, we may introduce the dimensionless variables:

$$r' = \frac{r}{L}, \quad z' = \frac{z}{H}, \quad u' = \frac{U}{L}, \quad w' = \frac{w}{W}, \quad t' = \frac{tW}{H}.$$

If the ratio of length scales is denoted ε, with the continuity equation [11], we can write:

$$\varepsilon = \frac{H}{L} = \frac{W}{U}. \qquad [14]$$

If P is the characteristic pressure in the film, the continuity and the Navier–Stokes equations are rewritten as:

$$\frac{1}{r'}\frac{\partial(u'r')}{\partial r'} + \frac{\partial w'}{\partial z'} = 0, \qquad [11']$$

$$\frac{\partial u'}{\partial t'} + u'\frac{\partial u'}{\partial r'} + w'\frac{\partial u'}{\partial z'} = -\frac{\varepsilon^2 P}{\rho W^2}\frac{\partial p'}{\partial r'} + \frac{\varepsilon}{\mathrm{Re}}\left[\frac{\partial}{\partial r'}\left(\frac{1}{r'}\frac{\partial(r'u')}{\partial r'}\right) + \frac{1}{\varepsilon^2}\frac{\partial^2 u'}{\partial z'^2}\right] \qquad [12']$$

and

$$\frac{\partial w'}{\partial t'} + u'\frac{\partial w'}{\partial r'} + w'\frac{\partial w'}{\partial z'} = -\frac{P}{\rho W^2}\frac{\partial p'}{\partial z'} + \frac{\varepsilon}{\mathrm{Re}}\left(\frac{\partial^2 w'}{\partial r'^2} + \frac{1}{r'}\frac{\partial w'}{\partial r'} + \frac{1}{\varepsilon^2}\frac{\partial^2 w'}{\partial z'^2}\right), \qquad [13']$$

with the Reynolds number

$$\mathrm{Re} = \frac{\rho WL}{\mu} = \frac{\rho UH}{\mu}.$$

In the lubrication approximation, if L is the film radius R_f and H is the initial film thickness, it is assumed $\varepsilon \ll 1$ and $\mathrm{Re} \ll 1$. The characteristic pressure P can be taken as (Ivanov & Dimitrov 1988):

$$P = \frac{\mu UL}{H^2}. \qquad [15]$$

Thus, [12′] becomes

$$\frac{\partial u'}{\partial t'}+u'\frac{\partial u'}{\partial r'}+w'\frac{\partial u'}{\partial z'}=\frac{1}{\varepsilon \mathrm{Re}}\left[-\frac{\partial p'}{\partial r'}+\frac{\partial^2 u'}{\partial z'^2}+\varepsilon^2\frac{\partial}{\partial r'}\left(\frac{1}{r'}\frac{\partial(r'u')}{\partial r'}\right)\right]. \quad [16]$$

The asymptotic value is given by

$$-\frac{\partial p'}{\partial r'}+\frac{\partial^2 u'}{\partial z'^2}=0. \quad [17]$$

With the same approximation, [13′] is reduced to

$$\frac{\partial p'}{\partial z'}=0. \quad [18]$$

Equations [17] and [18] constitute the classical frame for studying the drainage of viscous films. But the rate of drainage predicted by such an analysis is too low when compared with the experimental results for the collision of two bubbles or for the impact of a bubble with a free surface. Therefore the formulation of the film drainage must be re-examined.

During the stage of film formation, the characteristic pressure is the capillary pressure $P_c=\gamma/R$. The axial velocity is scaled by the relative approach velocity V_0. The radial characteristic length L is given by the film radius R_m when the bubbles are in contact. For a bubble of radius R_b resting in equilibrium at a free surface, R_m is given by (Princen 1963):

$$R_m^2=\frac{4}{3}\frac{\Delta\rho g}{\gamma}R_b^4. \quad [19]$$

In this case, it will be shown that the initial film thickness h_0, [44], is of the order of

$$H_i=\frac{\rho V_\infty^2 R_b^2}{\gamma}, \quad [20]$$

if the terminal velocity V_∞ is taken as the relative approach velocity.

With a Reynolds number,

$$\mathrm{Re}_f=\frac{\rho V_0 R_m}{\mu}, \quad [21]$$

and a Weber number,

$$\mathrm{We}=\frac{\rho V_0^2 R_b}{\gamma}, \quad [22]$$

the Navier–Stokes equations may be written as

$$\frac{\partial u'}{\partial t'}+u'\frac{\partial u'}{\partial r'}+w'\frac{\partial u'}{\partial z'}=-\frac{\varepsilon^2}{\mathrm{We}}\frac{\partial p'}{\partial r'}+\frac{\varepsilon}{\mathrm{Re}_f}\left[\frac{\partial}{\partial r'}\left(\frac{1}{r'}\frac{\partial(r'u')}{\partial r'}\right)+\frac{1}{\varepsilon^2}\frac{\partial^2 u'}{\partial z'^2}\right] \quad [23]$$

and

$$\frac{\partial w'}{\partial t'}+u'\frac{\partial w'}{\partial r'}+w'\frac{\partial w'}{\partial z'}=-\frac{1}{\mathrm{We}}\frac{\partial p'}{\partial z'}+\frac{\varepsilon}{\mathrm{Re}_f}\left(\frac{\partial^2 w'}{\partial r'^2}+\frac{1}{r'}\frac{\partial w'}{\partial r'}+\frac{1}{\varepsilon^2}\frac{\partial^2 w'}{\partial z'^2}\right). \quad [24]$$

In our experiments, H_i and R_m have the same magnitude. For example, with a bubble of radius $R_b=0.4$ mm, rising in water, the terminal velocity is 20 cm/s and $R_m=68\,\mu$m, $H_i=88\,\mu$m, $\mathrm{Re}_f=13.6$ and $\mathrm{We}=0.22$. Therefore, during the initial stage of drainage, taking $H=h_0$, ε is of the order of unity and $\mathrm{We}/\mathrm{Re}\ll 1$. Consequently, the viscous terms in the Navier–Stokes equations are of minor importance, unlike the lubrication approximation.

We assume now that the radial velocity is uniform across the film [hypothesis (e)]. As discussed by Lee & Hodgson (1968), the velocity profile is determined by the tangential part of the stress tensor at the film surface. Neglecting the influence of the gas phase due to its low viscosity

[hypothesis (d)] and the effect of a surface viscosity, the surface stress balance equation is in a radial direction:

$$\mu\left(\frac{\partial u}{\partial z}+\frac{\partial w}{\partial r}\right)_{z=\pm h/2}=\frac{\partial \gamma}{\partial r}. \qquad [25]$$

The gradient of interfacial tension is related to the variation of the surface concentration of the surface-active molecules. If the gradient $\partial\gamma/\partial r$ is small, the film will be slightly sheared. So we can consider

$$\frac{\partial \gamma}{\partial r}=0 \qquad [26]$$

and

$$\frac{\partial u}{\partial z}=0, \qquad [27]$$

not only at the surface but in the whole film as for a plug flow.

The Navier–Stokes equations become

$$\frac{\partial u'}{\partial t'}+u'\frac{\partial u'}{\partial r'}=-\frac{\varepsilon^2}{\mathrm{We}}\frac{\partial p'}{\partial r'}+\frac{\varepsilon}{\mathrm{Re_f}}\left[\frac{\partial}{\partial r'}\left(\frac{1}{r'}\frac{\partial (r'u')}{\partial r'}\right)\right] \qquad [28]$$

and

$$\frac{\partial w'}{\partial t'}+u'\frac{\partial w'}{\partial r'}+w'\frac{\partial w'}{\partial z'}=-\frac{1}{\mathrm{We}}\frac{\partial p'}{\partial z'}+\frac{\varepsilon}{\mathrm{Re_f}}\left(\frac{\partial^2 w'}{\partial r'^2}+\frac{1}{r'}\frac{\partial w'}{\partial r'}+\frac{1}{\varepsilon^2}\frac{\partial^2 w'}{\partial z'^2}\right). \qquad [29]$$

Integrating the continuity equation [11'] according to [27] and with $w'(r', 0, t')=0$, we obtain

$$w'=-\frac{z'}{r'}\frac{\partial (r'u')}{\partial r'}. \qquad [30]$$

The film being plane-parallel, for $z'=\pm h'/2$, we have

$$\frac{\mathrm{d}h'}{\mathrm{d}t'}=-\frac{h'}{r'}\frac{\partial (r'u')}{\partial r'}. \qquad [31]$$

Integrating [31] with $u'=0$ at $r'=0$,

$$u'=-\frac{r'}{2h'}\frac{\mathrm{d}h'}{\mathrm{d}t'}; \qquad [32]$$

and with [30],

$$w'=\frac{z'}{h'}\frac{\mathrm{d}h'}{\mathrm{d}t'}. \qquad [33]$$

Substituting [32] in the Navier–Stokes equation [28] and setting

$$\mathscr{H}=\tfrac{1}{2}\ln h', \qquad [34]$$

we observe that the viscosity term disappears in the momentum equation for the radial direction:

$$r'\left[-\frac{\mathrm{d}^2\mathscr{H}}{\mathrm{d}t'^2}+\left(\frac{\mathrm{d}\mathscr{H}}{\mathrm{d}t'}\right)^2\right]=-\frac{\varepsilon^2}{\mathrm{We}}\frac{\partial p'}{\partial r'}. \qquad [35]$$

This equation was given by Chesters (1975) who integrates [35] between $r'=0$ and $r'=1$ and evaluates the pressure at the film border. But this integration leads to a gradient of pressures in the radial direction, in contradiction with the hypothesis of a plane-parallel film. On the contrary, we assume that the Laplace law is verified at each point of the film surface. Writing the continuity of the normal component of the stress tensor for a plane interface:

$$p_b=p\left(\frac{h}{2}\right)-2\mu\left(\frac{\partial w}{\partial z}\right)_{h/2}, \qquad [36]$$

where p_b is the bubble pressure. If p_0 is the pressure in the bulk liquid,

$$p_b = p_0 + \frac{2\gamma}{R_b}.$$

With dimensionless variables, [36] becomes

$$p'_0 + 2 = p'\left(\frac{h'}{2}\right) - \frac{2\mathrm{We}}{\varepsilon \mathrm{Re}_f}\frac{\partial w'}{\partial z'}. \qquad [36']$$

If we assume p_b constant, we see that [33] and [36] imply

$$\frac{\partial p'}{\partial r'} = 0. \qquad [37]$$

Then equation [20] leads to

$$\frac{\mathrm{d}^2\mathscr{H}}{\mathrm{d}t'^2} = \left(\frac{\mathrm{d}\mathscr{H}}{\mathrm{d}r'}\right)^2. \qquad [38]$$

Integrating [23] with the initial conditions

$$t = \begin{cases} h = h_0 \\ \left(\dfrac{\mathrm{d}h}{\mathrm{d}t}\right)_{t=0} = -V_0; \end{cases} \qquad [39]$$

or for $t' = 0$: $h' = 1, \mathrm{d}h'/\mathrm{d}t' = 1, \mathscr{H} = 0, \mathrm{d}\mathscr{H}/\mathrm{d}t' = -\frac{1}{2}$, we obtain

$$h' = \frac{4}{(t'+2)^2}. \qquad [40]$$

In dimensional form,

$$h = \frac{4h_0^3}{(V_\infty t + 2h_0)^2}. \qquad [40']$$

Substituting [32], [33] and [40] in [29] and integrating [29] with the boundary condition [36], the film pressure is given by

$$p' - p'_0 = 2 + \frac{3\mathrm{We}}{4}h'\left(\frac{h'^2}{4} - z'^2\right) - \frac{2\mathrm{We}}{\varepsilon \mathrm{Re}_f}(h')^{1/2} \qquad [41]$$

or

$$p(r, z, t) = p_b + \frac{3\rho}{\tau^2}\frac{h}{h_0}\left(\frac{h^2}{4} - z^2\right) - \frac{4\mu}{\tau}\left(\frac{h}{h_0}\right)^{1/2}. \qquad [41']$$

where $\tau = 2h_0/V_0$.

Equation [40] satisfies the observed dependence [3] during the first stage of drainage, but initial conditions [39] are needed. An estimation of h_0 was given by Chesters (1978), who chose h_0 such that the pressure between two approaching spherical bubbles is of the order of the capillary pressure. He found that the pressure between two spheres of radius R approaching with relative velocity V_0 is on their centreline:

$$p_0 = \frac{\rho V_0^2 R}{4h_0}\left(1 + \frac{4\mu}{\rho V_0 R}\right). \qquad [42]$$

Then, following Chesters (1978), we have at the initial time,

$$p_0 = \frac{\gamma}{R} \quad \text{and} \quad \left(\frac{\mathrm{d}h}{\mathrm{d}t}\right)_{t=0} = -V_0; \qquad [43]$$

hence

$$h_0 = \frac{\rho V_0^2 R^2}{4\gamma}\left(1 + \frac{4\mu}{\rho V_0 R}\right). \qquad [44]$$

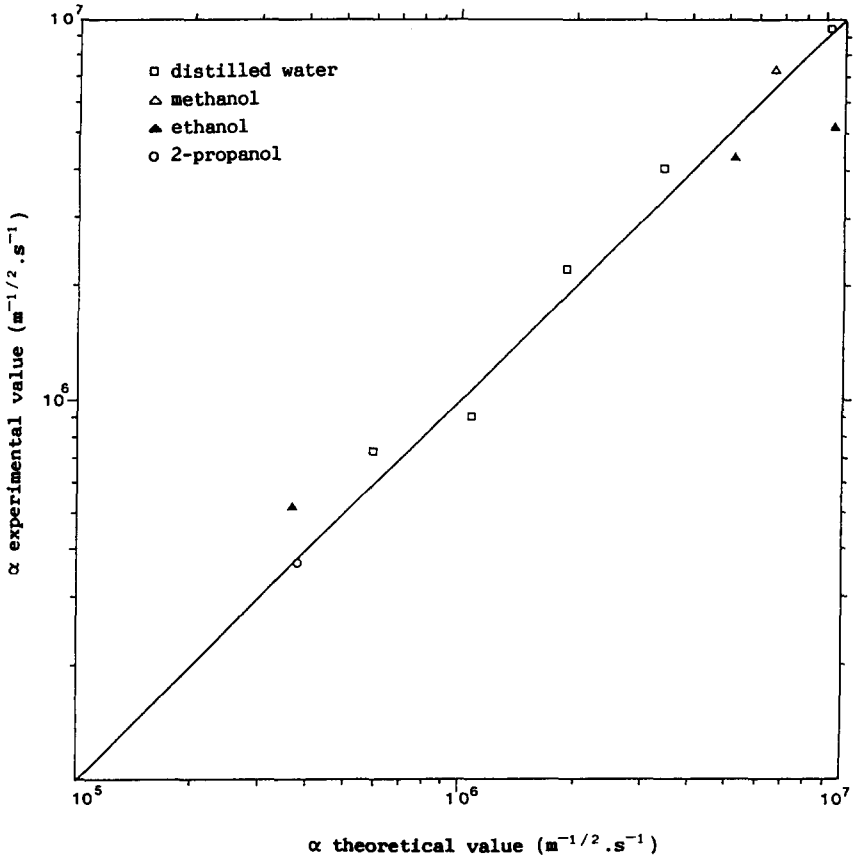

Figure 8. Comparison of experimental values of α with predicted values using [48].

For two unequally sized bubbles of radii R_1 and R_2, Chesters (1978) showed that the acceleration of the reference frame, with its origin taken at the film centre, can be neglected and the thinning equations are the same as those for equally sized bubbles provided that R is replaced by an equivalent radius R_{eq} given by [9].

For a bubble approaching a free surface $R_{eq} = 2R_b$, and if we assume that the relative velocity V_0 is the rise velocity V_∞ of the bubble, we can rewrite [40′] as

$$\frac{1}{\sqrt{h}} = \alpha_C(t + t_0), \qquad [45]$$

with

$$\alpha_C = \frac{1}{2V_\infty^2 R_b^3}\left[\frac{\gamma}{\rho\left(1 + \frac{2\mu}{\rho V_\infty R_b}\right)}\right]^{3/2} \qquad [46]$$

and

$$t_0 = \frac{2h_0}{V_\infty}. \qquad [47]$$

In fact, the best fit with experimental results is obtained if the numerical coefficient 1/2 is replaced by 4, such that

$$\alpha = \frac{4}{V_\infty^2 R_b^3}\left[\frac{\gamma}{\rho\left(1 + \frac{2\mu}{\rho V_\infty R_b}\right)}\right]^{3/2} \qquad [48]$$

Comparison of the experimental values with the proposed coefficient α, [48], are shown in figure 8 for small bubbles in several pure liquids (water, methanol, ethanol, 2-propanol). The uncertainty on experimental values of α is about 15% and the agreement is very good.

The difference between the numerical coefficients of [46] and [48] may be explained either by an initial relative velocity $< V_\infty$ or by an initial pressure $> \gamma/R$; the first case signifying that the bubble decelerates before film formation.

5. DISCUSSION

The main feature of this model is to omit in the Navier–Stokes equations the term $\partial u/\partial z$, as for a plug flow, and to assume there is no gradient of pressure in the radial direction. The first hypothesis follows from the continuity of tangential stress at the film surface. If the influence of gas flow and surface viscosity are neglected, the continuity of the tangential stress for a plane surface is expressed as

$$\mu\left(\frac{\partial u}{\partial z}\right)_{z=h/2} = \frac{\partial \gamma}{\partial r} = \frac{\partial \gamma}{\partial c}\frac{\partial c}{\partial r}, \qquad [49]$$

denoting by c the surfactant concentration at $z = \pm h/2$.

If $\partial c/\partial r \approx \Delta c/R_m$, where Δc is the concentration difference between the centre and the rim of the film, the order of $\partial u'/\partial z'$ is given by $(\varepsilon^2/\mu V_0)(\partial\gamma/\partial c)\Delta c$. In our experiments, the surfaces are clean so that the gradient $\partial\gamma/\partial r$ due to impurities is very small. For the ethanol solutions $\partial\gamma/\partial c = -2 \cdot 10^{-5}$ (N/mol) $\cdot$ m^2 (Butler 1932) and c is of the order of 3.5 mol/m^3. For a bubble rising with the velocity $V_0 = 20$ cm/s, if $\Delta c \approx 0.1$ mol/m^3 and $\varepsilon = 1$, $\partial u'/\partial z' < 0.01$. Therefore, the approximation of a plug flow seems justified initially.

Furthermore, it may be pointed out that $\partial\gamma/\partial r = 0$ is consistent with the model. If $\Delta\mathscr{A}$ is the film area found between r and $r + \Delta r$, then for a thickness variation of δh, the variation of $\Delta\mathscr{A}$ is

$$\frac{\delta(\Delta\mathscr{A})}{\Delta\mathscr{A}} = \frac{1}{r}\frac{\partial(r\delta r)}{\partial r} = -\frac{\delta h}{h}. \qquad [50]$$

Thus, the stretching $\delta(\Delta\mathscr{A})$ does not depend on r and the surfactant concentration may be uniform on the film surface.

The law $h^{-1/2} = \alpha t$ is valid only during the first stage of drainage. Two hypotheses can explain the end of the initial stage. The first is that the film thinning is related to the bubble motion: if the bubble dives after the bounce, the liquid flows into the film and drainage is stopped. The second hypothesis is the formation of a dimple, as was observed with viscous liquids by Allan *et al.* (1961). In this case, the thinning occurs at a greater rate at the rim of the film than at the centre, and the liquid is trapped within a ring.

Bouncing

When a bubble is floating at a free surface, Lu *et al.* (1989) have shown that it can oscillate according to two fundamentally different modes: the surface mode and the volume mode. The surface mode is given by the vertical oscillation of the bubble; the shape remains essentially constant and the restoring force is due to the deformation of the free surface. The volume mode is characterized by radial vibration of the bubble surface and the restoring force is provided by the compressibility of the gas contained in the bubble. Furthermore, their study has shown that the frequency of this second mode has the same order of magnitude as in an unbounded liquid:

$$\nu = \frac{1}{2\pi R_b}\left(\frac{3K}{\rho}p_b\right)^{1/2}, \qquad [51]$$

where K is the polytropic exponent of gas.

The periods of this mode are of the order of 0.1 ms for the bubbles examined here. They are clearly shorter than the characteristic time of drainage (1 ms) and this mode does not appear on the experimental curves of film drainage.

For the surface mode, Lu *et al.* (1989) gives only an estimate of the frequency and do not take into account the approach velocity of the bubble. This mode of oscillation has also been studied by Hartland *et al.* (1975), who calculated the numerical values of frequencies and amplitudes for solid spheres and drops at a fluid–liquid interface. For bubbles, the order of magnitude of the frequency for vertical oscillations can be given by a simple model, which we present below.

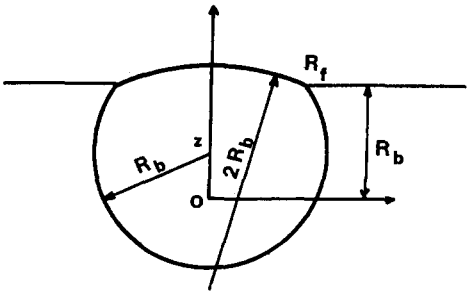

Figure 9. Schematic shape of a bubble oscillating at a free surface.

The simplified form of the bubble at the free surface is shown in figure 9. The bubble of volume $\mathscr{V}$ is divided into two spherical zones. The curvature radius of the lower part is R_b, while that of the upper part is $2R_b$ if we assume that the film pressure P_f is given by

$$P_f = P_b - \frac{\gamma}{R_b} = P_0 + \frac{\gamma}{R_b}, \qquad [52]$$

where P_b and P_0 signify the pressure inside and outside the bubble, respectively. The volume of the upper part is very small and the centre of the lower sphere is taken as the centre of mass. Taking the origin at a distance R_b from the horizontal free surface, the equation of motion is

$$m\frac{d^2z}{dt^2} = \Delta\rho g\mathscr{V} - \pi R_f^2\frac{\gamma}{R_b} - f\frac{dz}{dt}, \qquad [53]$$

where

$$m = C_m\rho\mathscr{V} \qquad [54]$$

is the added (virtual) mass of the bubble.

For a sphere in an unbounded volume, $C_m = 0.5$ and near a rigid wall $C_m = 11/16$ (Milne-Thompson 1962). Here we suppose that C_m does not depend on z. The first term on the r.h.s. of [53] is the buoyancy force. Neglecting the gas density, we take $\Delta\rho g\mathscr{V} = 4\pi\rho g R_b^3/3$.

The second term is the restoring force due to the excess of pressure acting on the film of radius R_f. From elementary geometry, R_f is given approximately by

$$R_f^2 = 2R_b z \quad \text{for } z > 0 \qquad [55a]$$

and

$$R_f = 0 \qquad \text{for } z < 0. \qquad [55b]$$

The last term of [53] is the drag force. If the drag coefficient C_D is given by (Kang & Leal 1988):

$$C_D = \frac{48}{Re_b} = \frac{8}{3}\frac{gR_b}{V_\infty^2}, \qquad [56]$$

with the Reynolds number

$$Re_b = \frac{2\rho V_\infty R_b}{\mu},$$

the friction coefficient f can be expressed by

$$f = 12\pi\mu R_b. \qquad [57]$$

Let us introduce the dimensionless variables

$$Z = \frac{z}{R_b} \quad \text{and} \quad t'' = \frac{tV_\infty}{R_b}. \qquad [58]$$

The equation of motion is, thus, for $Z > 0$:

$$C_m\frac{d^2Z}{dt''^2} = \frac{gR_b}{V_\infty^2} - \frac{3}{We}Z - \frac{18}{Re_b}\frac{dZ}{dt''}. \qquad [59]$$

The equilibrium position is given by

$$Z_0 = \frac{gR_b We}{3V_\infty^2} = \frac{2\rho g R_b^2}{3\gamma} = \frac{C_D We}{8}. \quad [60]$$

The corresponding film radius R_m is the same as that given by [19]:

$$\frac{R_m^2}{R_b^2} = 2Z_0. \quad [61]$$

Thus, the equation of motion [59] becomes

$$C_m \frac{d^2Z}{dt''^2} = \frac{3}{We}(Z_0 - Z) - \frac{18}{Re_b}\frac{dZ}{dt''}. \quad [62]$$

Denoting

$$\omega^2 = \frac{3}{C_m We}, \quad \beta = \frac{9}{C_m Re_b}, \quad \Omega^2 = \omega^2 - \beta^2, \quad [63]$$

and with the initial conditions $t'' = 0$: $Z = 0$, $dZ/dt'' = 1$, $d^2Z/dt''^2 = 0$, the solution of [62] is, for $Z > 0$:

$$Z_1(t'') = \exp(-\beta t'')\left[-Z_0\cos(\Omega t'') + \frac{\omega^2 - 2\beta^2}{\omega^2\Omega}\sin(\Omega t'')\right] + Z_0. \quad [64]$$

If, as in our experiments, $\beta^2 \ll \omega^2$, the pseudo-period is

$$T_1'' = 2\pi\sqrt{\frac{C_m We}{3}} \quad [65]$$

or in dimensional form,

$$T_1 = \sqrt{\frac{2\pi C_m \rho \mathscr{V}}{\gamma}}. \quad [65']$$

With $C_m = 11/16$, the bubble is emerging during

$$\frac{T_1}{2} \approx \sqrt{\frac{\rho\mathscr{V}}{\gamma}}.$$

For diameters varying between 0.54 and 0.85 mm, $T_1/2$ takes place between 1 and 2 ms. This is in accordance with the results shown in figure 7.

The bubble leaves the free surface at $t'' = t_1''$, given by $Z_1(t_1'') = 0$ with the velocity V_1''. Then it dives beneath the free surface and the equation of motion is, for $Z > 0$:

$$C_m \frac{d^2Z}{dt''^2} = \frac{18}{Re_b}\left(1 - \frac{dZ}{dt''}\right). \quad [66]$$

According to the initial conditions, the solution of [66] is

$$Z_2(t'') = \frac{1 - V_1''}{2\beta}\{\exp[-2\beta(t'' - t_1'')] - 1\} + t'' - t_1''. \quad [67]$$

The bubble returns to the surface at $t'' = t_2''$, given by $Z_2(t_2'') = 0$. With $V_1'' \approx -1$, the order of magnitude of $t_2'' - t_1''$ is $1/\beta$. For a bubble with a radius of 0.4 mm, the computed value of $t_2'' - t_1''$ is 25 ms, while the experimental value is about 15 ms (figure 3). Therefore, this model is only an approximation but it shows that the lifetime of the film t_1'' is short in comparison with the time of one oscillation t_2''. Consequently, the film drainage should be studied taking into account the bubble rebound.

Dimpling

Dimple formation has been chiefly studied in the frame of the lubrication approximation (Ivanov & Dimitrov 1988) or at least for the limiting case of small inertia: see Chi & Leal (1989), Ascoli *et al.* (1990), Pozrikidis (1990) and Yiantsios & Davis (1990) for drops. Shopov *et al.* (1990) have

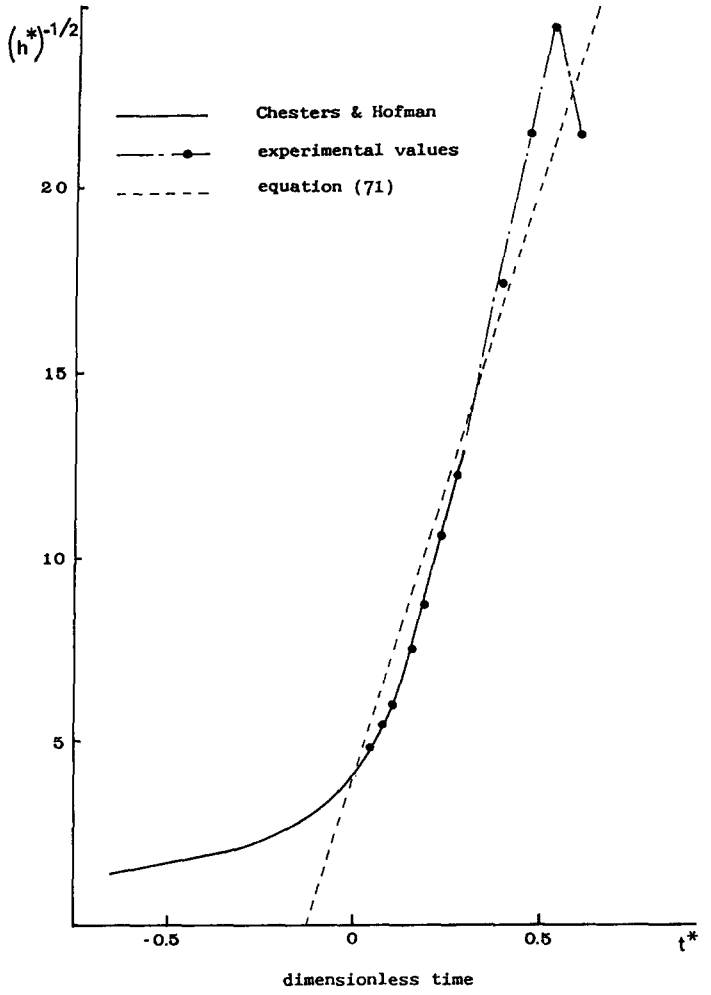

Figure 10. Comparison of the measured thicknesses h^* for a bubble of 0.54 mm dia (terminal velocity = 0.11 m/s) with the values computed by Chesters & Hofman (1982) at the film centre and with [70]. The origin of time is taken at $(h^*)^{-1/2} = 4$ for the three curves.

examined numerically a bubble approaching a rigid wall. The difficulty encountered in these works lies in coupling the small-scale film thinning process and the long-scale problem of the bubble (or drop) motion. It is often stated that the dimpling is related to the no-slip condition at the film surface. However, Yiantsios & Davis (1990) have shown that for a drop approaching a free surface, a dimple is always formed at sufficient long times.

Chesters & Hofman (1982) have examined numerically the case of the film formation during the collision of two bubbles. They assume uniform velocity across the film and full mobility of the surface. Therefore, their analysis is very similar to that of the analytical model presented here (section 4). Dimple formation is also observed. They showed that if the viscosity is neglected, it is possible to obtain a universal solution which does not depend on the Weber number (provided this is small). Their governing equations are only a function of the following variables:

$$r^* = \frac{r}{R_{eq}\,We^{1/2}}, \quad h^* = \frac{h}{R_{eq}\,We}, \quad u^* = \frac{u\,We^{1/2}}{V_\infty}, \quad t^* = \frac{tV_\infty}{R_{eq}\,We}, \qquad [68]$$

with $We = \rho V^2 R_{eq}/\gamma$. Denoting $\delta = h_0/R_{eq}$, with these variables, the drainage law [40] is rewritten as:

$$(h^*)^{-1/2} = \frac{1}{2}\left(\frac{We}{\delta}\right)^{3/2} t^* + \left(\frac{We}{\delta}\right)^{1/2}. \qquad [69]$$

Hence this expression does not depend on We if $\delta \propto We$. This is verified by [44], which gives for the inviscid case $h_0^* = \delta/We = 1/4$. For a bubble approaching a free surface ($R_{eq} = 2R_b$), using [48], a better fit with the experimental results is obtained taking $h_0^* = 1/16$. Then the numerical results of Chesters & Hofman (1982) can be compared with

$$(h^*)^{-1/2} = 32t^* + 4. \quad [70]$$

The onset of dimpling is predicted, by these authors, to occur at about $h^* = 10^{-2}$, corresponding to 0.5, 2, 3 and 5 μm for the four bubbles denoted **a**, **b**, **c** and **d**, respectively, in figure 7. Except for the smaller bubble, the dimple should already be established when the thickness measurements start. Hence, from this simulation, it seems that the end of the initial stage of drainage is not due to a dimple formation.

In figure 10, the thickness at the film centre computed by Chesters and Hofman (1982) is compared with the experimental values and with [70] for the smaller bubble **a**. The accordance with the experimental results is very satisfactory up to the last computed value $h^* = 6 \cdot 10^{-3}$. However, for this value, the thickness at the rim is given as $h^* = 4.8 \cdot 10^{-4}$ ($h = 23$ nm). This is the order of magnitude of the rupture thickness and in reality the drainage continues as far as $h^* = 1.6 \cdot 10^{-3}$ ($h = 80$ μm) at the film centre. The comparison with the other bubbles also shows that the drainage is observed for longer than predicted by the simulation. Furthermore, this simulation does not take into account the bubble deceleration. Therefore, the end of the initial phase of drainage is not yet well-explained and a more accurate analysis of the drainage at the rim is needed to understand the rupture.

6. CONCLUSION

The examination of the drainage curves for distilled water and alcoholic solutions shows that the inhibition of coalescence by alcohol cannot be explained by a slower rate of thinning in the central region of the film. The addition of alcohol acts to prevent the film rupture. This rupture does not occur when the thickness at the film center is a minimum, but later when liquid flows into the film. The rupture is abrupt; we do not observe growth of instabilities beforehand.

For the first stage of drainage, we propose a modification of the Chesters (1975) model which gives a good agreement with the experimental drainage curves. But further development of the theory is needed to explain the effect of alcohol on the film rupture.

REFERENCES

ALLAN, R. S., CHARLES, G. E. & MASON, S. G. 1961 The approach of gas bubbles to a gas/liquid interface. *J. Colloid Sci.* **16,** 150–165.

ANDREW, S. P. S. 1960 Frothing in two-component liquid mixtures. In *Proc. Int. Symp. on Distillation*, pp. 73–78. Instn Chem. Engrs, London.

ASCOLI, E. P., DANDY, D. S. & LEAL, L. G. 1990 Buoyancy-driven motion of a deformable drop toward a planar wall at low Reynolds number. *J. Fluid Mech.* **213,** 287–311.

BUTLER, J. A. V. & WIGHTMAN, A. 1932 Adsorption at the surface of solutions. Part I. The surface composition of water–alcohol solutions. *J. Chem. Soc.* 2089–2097.

CAIN, F. W. & LEE, J. C. 1985 A technique for studying the drainage and rupture of instable liquid films formed between two captive bubbles: measurements on KCl solutions. *J. Colloid Interface Sci.* **106,** 70–85.

CHEN, J. D. & SLATTERY, J. C. 1988 Effects of electrostatic double-layer forces on coalescence. *AIChE Jl* **34,** 140–143.

CHESTERS, A. K. 1975 The applicability of dynamic-similarity criteria to isothermal, liquid–gas, two phase flows without mass transfer. *Int. J. Multiphase Flow* **2,** 191–212.

CHESTERS, A. K. 1978 Fundamental problems in gas–liquid two-phase flow. Ph.D. Thesis, Delft Univ. of Technology, The Netherlands.

CHESTERS, A. K. & HOFMAN, G. 1982 Bubble coalescence in pure liquids. *Appl. scient. Res.* **38,** 353–361.

CHI, B. K. & LEAL, L. G. 1989 A theoretical study of the motion of a viscous drop toward a fluid interface at low Reynolds number. *J. Fluid Mech.* **201,** 123–146.

COUALALOGLOU, C. A. & TAVLARIDES, L. L. 1977 Description of interaction processes in agitated liquid–liquid dispersions. *Chem. Engng Sci.* **32,** 1289–1297.

DAS, P. K., KUMAR, R. & RAMKRISHNA, D. 1987 Coalescence of drops in stirred dispersion. A white noise model for coalescence. *Chem. Engng Sci.* **42,** 213–220.

DAVIS, R. H., SCHONBERG, J. A. & RALLISON, J. M. 1989 The lubrication force between two viscous drops. *Phys. Fluids* **A1,** 77–81.

DROGARIS, G. & WEILAND, P. 1983 Studies of coalescence of bubble pairs. *Chem. Engng Commun.* **23,** 11–26.

FAROOQ, S. Y. 1972 Ph.D. Thesis, Univ. of Wales, Swansea, U.K.

HAHN, P. S., CHEN, J. D. & SLATTERY, J. C. 1985 Effects of London–van der Waals forces on the thinning and rupture of a dimpled liquid film as a small drop or bubble approaches a fluid–fluid interface. *AIChE Jl* **31,** 2026–2038.

HARTLAND, S., RAMAKRISHNAN, S. & HARTLEY, R. W. 1975 The oscillation of drops and spheres at fluid–liquid interfaces. *Chem. Engng Sci.* **30,** 1141–1148.

IVANOV, I. B. (Ed.) & DIMITROV, D. S. 1988 Thin film drainage. In *Thin Liquid Films*, pp. 379–496. Dekker, New York.

KANG, I. S. & LEAL, L. G. 1988 The drag coefficient for a spherical bubble in a uniform streaming flow. *Phys. Fluids* **31,** 233–237.

KEITEL, G. & ONKEN, U. 1982 The effect of solutes on bubble size in air–water dispersions. *Chem. Engng Commun.* **17,** 85–98.

KIM, J. W. & LEE, W. K. 1988 Coalescence behavior of two bubbles growing side-by-side. *J. Colloid Interface Sci.* **123,** 303–305.

KIRKPATRICK, R. D. & LOCKETT, M. J. 1974 The influence of approach velocity on bubble coalescence. *Chem. Engng Sci.* **29,** 2363–2373.

LEE, J. C. & HODGSON, T. D. 1968 Film flow and coalescence. *Chem. Engng Sci.* **23,** 1375–1397.

LESSARD, R. R. & ZIEMINSKI, S. A. 1971 Bubble coalescence and gas transfer in aqueous electrolytic solutions. *Ind. Engng Chem. Fundam.* **10,** 260–269.

LU, N. Q., OGUZ, H. N. & PROSPERETTI, A. 1989 The oscillations of a small floating bubble. *Phys. Fluids* **A1,** 252–260.

MANEV, E. D., SAZDANOVA, S. V. & WASAN, D. T. 1984 Emulsion and foam stability—the effect of film size on film drainage. *J. Colloid Interface Sci.* **97,** 591–594.

MARRUCCI, G. 1969 A theory of coalescence. *Chem. Engng Sci.* **24,** 975–985.

MILNE-THOMSON, L. M. 1962 *Theoretical Hydrodynamics*, Chap. XVI. Macmillan, New York.

NICODEMO, L., MARRUCCI, G. & ACIERNO, D. 1972 Bubble pair coalescence in electrolyte solutions. *Quad. Ing. Chim. Ital.* **8,** 1–7.

OOLMAN, T. O. & BLANCH, H. W. 1986 Bubble coalescence in stagnant liquids. *Chem. Engng Commun.* **43,** 237–261.

POZRIKIDIS, C. 1990 The deformation of a liquid drop moving normal to a plane wall. *J. Fluid Mech.* **215,** 331–363.

PRINCE, M. J. & BLANCH, H. W. 1990a Transition electrolyte concentrations for bubble coalescence. *AIChE Jl* **36,** 1425–1429.

PRINCE, M. J. & BLANCH, H. W. 1990b Bubble coalescence and breakup in air sparged bubble columns. *AIChE Jl* **36,** 1485–1499.

PRINCEN, H. M. 1963 Shape of a fluid drop at a liquid–liquid interface. *J. Colloid Sci.* **18,** 178–195.

RUCKENSTEIN, E. & SHARMA, A. 1987 A new mechanism of film thinning enhancement of Reynolds velocity by surface waves. *J. Colloid Interface Sci.* **119,** 1–13.

SAGERT, N. H., QUINN, M. J., CRIBBS, S. C. & ROSINGER, E. L. J. 1976 Bubble coalescence in aqueous solutions of *n*-alcohols. In *Foams; Proc. Symp.* (Edited by AKERS, R. J.), pp. 147–162. Academic Press, New York.

SCHELUDKO, A. 1967 Thin liquid film. *Adv. Colloid Interface Sci.* **1,** 391–464.

SHARMA, A. & RUCKENSTEIN, E. 1987 Critical thickness and lifetime of foams and emulsions: role of surface wave-induced thinning. *J. Colloid Interface Sci.* **119,** 14–29.

SHOPOV, P. J., MINEV, P. D., BAZHLEKOV, I. B. & ZAPRYANOV, Z. D. 1990 Interaction of a deformable bubble with a rigid wall at moderate Reynolds numbers. *J. Fluid Mech.* **219,** 241–271.

THOMAS, R. M. 1981 Bubble coalescence in turbulent flows. *Int. J. Multiphase Flow* **7,** 709–717.

YANG, Y. M. & MAA, J. R. 1984 Bubble coalescence in dilute surfactant solutions. *J. Colloid Interface Sci.* **123,** 120–125.

YIANTSIOS, S. G. & DAVIS, R. H. 1990 On the buoyancy-driven motion of a drop towards a rigid surface or a deformable interface. *J. Fluid Mech.* **127,** 547–573.

ZIEMINSKI, S. A. & WHITTEMORE, R. C. 1971 Behavior of gas bubbles in aqueous electrolyte solutions. *Chem. Engng Sci.* **26,** 509–520.